NUCLEAR SCIENCE AND TECHNIQUES **26**, 040303 (2015)

# Adsorption of gaseous iodine-131 at high temperatures by silver impregnated alumina*

CHENG Qing-Hui (程庆辉), LI Ze-Jun (李泽军), and CHU Tai-Wei (褚泰伟)†
*National Laboratory for Molecular Sciences, Radiochemistry and Radiation Chemistry Key Laboratory of Fundamental Science,*
*College of Chemistry and Molecular Engineering, Peking University, Beijing 100871, China*

(Received April 8, 2014; accepted in revised form April 16, 2014; published online August 11, 2015)

To prevent radioactive iodides from releasing into the environment in an accident of a nuclear power plant, silver-impregnated alumina ($Ag/Al_2O_3$) was fabricated, and its performance of radioactive iodine adsorption from high-temperature gas was tested. The silver loadings on alumina were obtained by ICP-OES and the texture properties of $Ag/Al_2O_3$ were characterized by $N_2$ adsorption-desorption. The $Ag/Al_2O_3$ was of reduced specific surface (107.2 $m^2/g$ at 650 °C). Crystalline phases of $Ag/Al_2O_3$ were confirmed through XRD characterization. After calcination at 650 °C for 2 h, the crystalline phase of $Ag/Al_2O_3$ changed. The $^{131}I$- removal efficiency of $Ag/Al_2O_3$ was tested at 100, 250, 350, 450 and 650 °C, with good decontamination factor values for the radioactive iodine. Silver-impregnated alumina can be applied as adsorbents to remove radioactive iodine at high temperatures in nuclear accident.

Keywords: Silver impregnated alumina, High temperature, Radioactive iodine, Adsorption, Decontamination factor

DOI: 10.13538/j.1001-8042/nst.26.040303

## I. INTRODUCTION

Nuclear energy has been exploited as an alternative to maintain energy sustainability for a half century, while environmental pollution caused by nuclear power plants (NPP) has become a worldwide concern [1, 2], especially in a sever accident of NPPs [3]. In March 2011, large amounts of nuclear dusts were released from Japan's Fukushima Daiichi NPPs due to failure of cooling systems in a huge earthquake and tsunami. Due to their high mobility, the most dangerous nuclides released in an NPP disaster are gaseous $^{85}Kr$ and $^{135}Xe$, and volatile $^{131}I$, $^{129}I$, $^{134}Cs$ and $^{137}Cs$, with extensive radioactive hazard to the public [4, 5]. Among them, $^{131}I$ ($t_{1/2} = 8.02\,d$) is the most harmful radionuclide because of its large quantity of release in a nuclear disaster and relatively high activities, and its high accumulation in human thyroid and further damage to organs if ingested; whereas $^{129}I$, which decays in a half-life of $1.57 \times 10^7$ a and emits lower energy beta-rays, would do nearly no harm to people [6, 7]. In early stages of the Fukushima Daiichi NPP disaster, gaseous $^{131}I$ released into the environment was estimated at $1.5 \times 10^{17}$ Bq [8–10]. Therefore, how to remove $^{131}I$ is an important research subject for safeguarding NPPs and the environment.

Great research efforts have been made to prepare adsorbents for $^{131}I$ removal, such as carbon-based materials [11–13], silica gel [14, 15], polymer resin [16], titanium based materials [17–20], cyclodextrin [21], molecular sieves [22–24], etc. Also, impregnants have been exploited to improve performance of adsorbents for iodide removal, such as KI [25, 26], TEDA [27, 28] and silver salts [29]. However, most researchers focus mainly on iodide removal from water or gases at low temperatures. Given the fact that an NPP in lost-of-coolant accident is in high temperatures [4], preparation of materials for adsorbing radioactive iodides at high temperatures is meaningful [30].

Alumina is widely applied to manufacture ceramic materials and catalyst supports due to its good heat-resisting properties and large specific surface area [31–33]. In consideration of high affinity between silver and iodide, silver based alumina was exploited in this work as an adsorbent for radioactive iodine at high temperatures.

## II. EXPERIMENTAL SECTION

### A. Reagents and instruments

Potassium iodate (A.R.): Shantou West Long Chemical Co., Ltd; potassium iodide (A.R.): Beijing Tongguang Fine Chemicals Company; $Na^{131}I$: HTA CO., Ltd.; L-(+)-tartaric acid (A.R.): Sinopharm Chemical Reagent Co., Ltd.; light petroleum (boiling range of 30–60 °C, A.R.): Beijing Chemical Works; $N_2$ (high purity): Beijing AP BAIF Gases Industry Co., Ltd.; nitrate silver (A.R.): Beijing Chemical Works; Alumina (neutral, 100–200 meshes): Sinopharm Chemical Reagent Co., Ltd.; nitric acid (A.R.): Shantou West Long Chemical Co., Ltd.

Tube furnace: Beijing Zhongshiyida Science and Technology Ltd.; KL-602 micro-injection pump: Beijing Kelly Med Co., Ltd.; D07-7B mass flow controller: Beijing Seven star Electronics Co., Ltd.; D08-1F flow displayer: Beijing Seven Star Electronics Co., Ltd.; XMT series digital display apparatus: Yuyao Jindian Instruments Co., Ltd.; quartz tube ($\Phi$12 mm × 620 mm): Beijing Haiqing Photoelectric Glass Instrument Co., Ltd.; ICP-OES (Prodigy): Leeman Labs; XRD (X'PERT-MRD): Phlips; injector (10 mL): Changzhou Yuekang Medical Appliance Co., Ltd.; ASAP2010 accelerated surface area and porosimetry analyzer: Micromeritics; 2470 WIZARD2 automatic gamma counter: Perkin Elmer; FH463A automatic scaler: Beijing Nuclear Instrument Fac-

---

* Supported by National Natural Science Foundation of China (No. 21201013)

† Corresponding author, twchu@pku.edu.cn

tory; disposable plastic tube (WG, $\Phi$10–12 mm × 75 mm): Zhejiang Plasmed Medical Technology Co., Ltd.

### B. Preparation of adsorbent

Silver based alumina was fabricated by the method of impregnation. Alumina was calcined at 450 °C for 2 h in a muffle furnace, and allowed to cool in a desiccator. Then, an appropriate amount of alumina was added into nitric silver solution in a light-shading flask at 80 °C. After 24 h, the as-samples were spun to dry and placed in an oven at 120 °C for 2 h, before a 2-h calcination at 450 °C in the muffle furnace. Finally the adsorbent was prepared, and $Ag/Al_2O_3$ of different calcination temperatures are accordingly marked as “$Ag/Al_2O_3$ ($T$°C / $t$ h)”, where $T$ is calcination temperature and $t$ is calcination time.

### C. Silver loadings on alumina

Silver loadings on alumina were analyzed by inductively coupled plasma (ICP). Small amounts of the as-prepared $Ag/Al_2O_3$ were mixed with concentrated nitric acid in a flask for 24 h. The filtrate was gathered into a volumetric flask and the silver loadings were confirmed about 10 wt.%.

### D. Characterization of adsorbents

Texture properties of the adsorbents were checked by the method of $N_2$ adsorption and desorption on Micromeritics ASAP2010 analyzer. Adsorbents were degassed in advance at 300 °C for 2 h. Specific surface areas of adsorbents were measured by the BET method (Brunauer, Emmett and Teller); and the average pore volume was calculated by the BJH method (Barrett, Joyner and Halenda).

To confirm their crystalline phases and check their heat-resisting properties, $Ag/Al_2O_3$ of different temperatures were characterized by X-ray diffraction (D/max-2500/PC X-ray diffractometer, Rigaku, Japan), using Cu $K_\alpha$ (the XRD system was operated at 45 kV and 40 mA). The samples were scanned in 0.01° steps from $2\theta = 10°$ to 80°, with the scan rate of $5° min^{-1}$.

### E. Adsorption of radioactive iodine

#### *1. Effect of temperature*

In this section, $Ag/Al_2O_3$ and $Al_2O_3$ were tested to evaluate their efficiency of $^{131}I$ removal at 100, 250, 350, 450 and 650 °C. Before the test, adsorbents were calcined at 450 °C for 2 h in the muffle furnace.

With trace amount of $^{131}I$, $I_2$ was prepared using 2 mL of 2% $KIO_3$ and 4 mL of 166 µg/mL KI (plus 1 mL $Na^{131}I$), with 1 mL of 5% *L*-(+)-tartaric acid as acid medium. The $I_2$ was dissolved in light petroleum. The $^{131}I$ radioactivity in a test was 0.1–2.0 MBq.

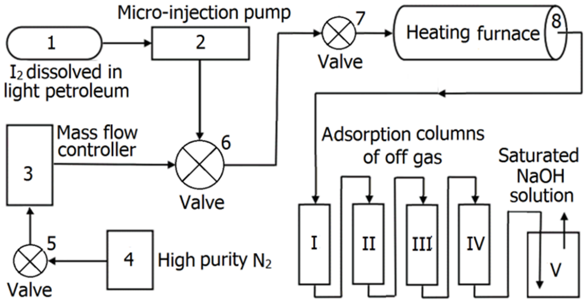

Fig. 1. Flow chart of the experiment.

The experimental apparatus (Fig. 1) consisted of the $^{131}I$-injection, heating and off gas purification sections. Radioactive iodine solution was injected by micro-injection pump in 2.5 mL/h of injection rate. High purity $N_2$ at a flow rate of 35 mL/min was used as carrier gas. In the experiment, the adsorbents were laterally loaded in the tube center to adsorb $^{131}I$ at different temperatures. A typical test with 1 g adsorbents in 5 mL light petroleum was done in 2 h. 13X (including Ag/13X zeolites, less than 40 meshes) and saturated NaOH solution were used to trap $^{131}I$ in the off gas [30]. After test, the spent adsorbents were imbedded in the disposable plastic tubes to detect radioactivity on the gamma counter. The decontamination factor were calculated by $DF = (A + B)/B$, where $A$ is the radioactivity of spent adsorbents and $B$ is the summation of radioactivities of the off gas purification columns. The *DF* values were normalized to $\lg DF/g$.

#### *2. Effect of $I_2$ concentration*

To study whether $I_2$ concentration would influence $^{131}I$-adsorbing performance of adsorbents, the KI concentration used as the source to produce iodine, was increased to 332 µg/mL, other details were the same as above.

#### *3. Effect of $N_2$ flow rate*

Considering that the flow rate of carrier gas may affect $^{131}I$ removal, $N_2$ flow rates of 15–75 mL/min were used to measure the removal efficiency of adsorbents at 250 °C. Other details were the same as above.

#### *4. Effect of adsorption time*

To check time-depenence of the interaction between $Ag/Al_2O_3$ and iodine, *DF* values in interaction durations of 30–180 min were measured at 100 °C and 450 °C under the $N_2$ flow rate of 35 mL/min. Iodine (dissolved in light petroleum) produced by the KI (166 µg/mL, $Na^{131}I$-included) was kept in a glass container. The amount of $Ag/Al_2O_3$ is about 1 g. As an example, the *DF* value of 30-min time point was measured as follows. Iodine dissolved in light petroleum was constantly injected by the micro-injection pump at 2.5 mL/h for 30 min, and radioactivity of the adsorbed $^{131}$I was measured to calculate the *DF* values.

## III. RESULTS AND DISCUSSION

### A. Adsorbents characterization

#### 1. *Texture properties of Ag/Al$_2$O$_3$*

Texture properties of adsorbents and support were characterized by the method of $N_2$ adsorption-desorption at 77 K. Figure 2 shows the $N_2$ isotherms of alumina, Ag/Al$_2$O$_3$ (450 °C/2 h) and Ag/Al$_2$O$_3$ (450 °C/2 h + 650 °C/2 h). The alumina maintained a mesoporous structure, which was in accordance with the calculation results by BJH method (average pore diameter of 4.5 nm). After loading silver on alumina, the Ag/Al$_2$O$_3$ (450 °C/2 h) and Ag/Al$_2$O$_3$ (450 °C/2 h + 650 °C/2 h) were still of the mesoporous structure, with an average pore diameter of 5.2 and 6.4 nm (BJH method), showing a little increase after silver loading. An adsorption hysteresis occurred when the relative pressure ($p/p_0$) reached to 1, i.e., all $N_2$ isotherms were attributed to Type IV.

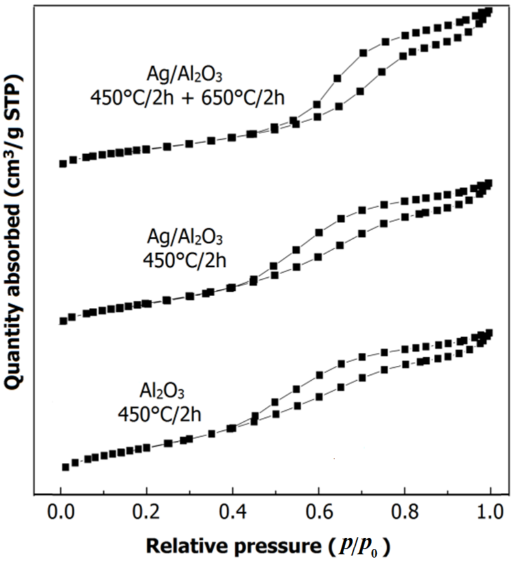

Fig. 2. $N_2$ adsorption-desorption isotherms of different adsorbents.

As shown in Table 1, the Ag/Al$_2$O$_3$ samples were of relatively large specific surface area, being 129.1 m$^2$/g and 107.2 m$^2$/g after 450 °C/2 h and 650 °C/2 h calcinations, respectively, though they were smaller than that of Al$_2$O$_3$.

TABLE 1. Texture properties of Al$_2$O$_3$ and Ag/ Al$_2$O$_3$

| Adsorbents | $S_{\mathrm{BET}}$ (m/g$^2$) |
|---|---|
| Al$_2$O$_3$(450 °C/2 h) | 146.1 |
| Ag/Al$_2$O$_3$(450 °C/2 h) | 129.1 |
| Ag/ Al$_2$O$_3$ (450 °C/2 h + 650 °C/2 h) | 107.2 |

#### 2. *XRD spectra of adsorbents*

Silver impregnated alumina had the characteristic diffraction peaks of alumina from the XRD spectrum (Fig. 3), i.e., it maintained a stable structure after silver impregnated. To be specific, silver on alumina had nearly no effect on the alumina structure. In the XRD spectrum of Ag/Al$_2$O$_3$ after 450 °C/2 h calcination, the diffraction peaks of silver particles can be seen clearly. For Ag/Al$_2$O$_3$ (450 °C/2 h + 650 °C/2 h), the crystalline phase of alumina changed, and the Ag diffraction peaks indicate sintering of the silver particles during the 2-h calcination at 650 °C.

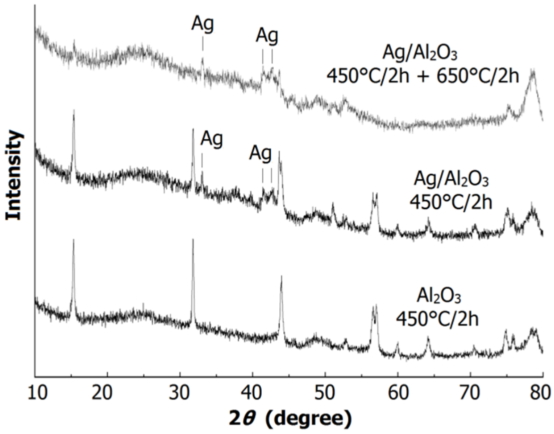

Fig. 3. XRD spectra of Al$_2$O$_3$ and Ag/Al$_2$O$_3$.

### B. Adsorption of radioactive iodine

#### 1. *Effect of adsorption temperature on $^{131}$I-removal efficiency*

The silver-impregnated alumina performs better in $^{131}$I-removal than alumina at the same temperatures under $N_2$ flow rate of 35 mL/min. As shown in Fig. 4, the $^{131}$I-removal efficiencies of both Al$_2$O$_3$ and Ag/Al$_2$O$_3$ decrease with increasing temperature of adsorption. However, *DF* values of the silver-impregnated alumina were 806.9 at 450 °C and 306.7 at 650 °C; while the *DF* values of alumina declined rapidly from 437.8(250 °C) to 16.1(650 °C).

Despite its reduced specific surface area (107.2 m$^2$/g for Ag/Al$_2$O$_3$, while 146.1 m$^2$/g for alumina), Ag/Al$_2$O$_3$ has higher *DF* value, as the silver particles can react with iodine from high-temperature gas to form AgI.

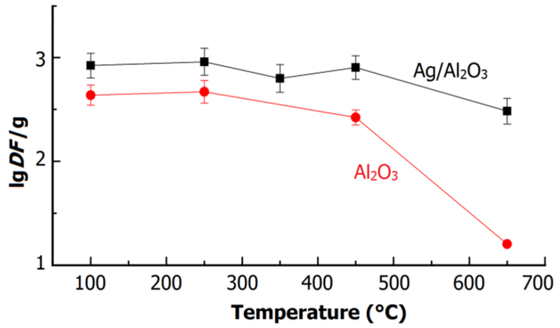

Fig. 4. (Color online) Adsorption of $^{131}$I at different temperatures by $Al_2O_3$ and $Ag/Al_2O_3$ under $N_2$ flow rate of 35 mL/min.

### 2. *Effect of $I_2$ concentration on removal efficiency*

$I_2$ concentrations of 166 µg/mL and 332 µg/mL were used to study the $I_2$ effect of dose on $^{131}$I-adsorbing performance of the $Ag/Al_2O_3$ at $N_2$ flow rate of 35 mL/min. The results are shown in Fig. 5. The $Ag/Al_2O_3$ was of high $^{131}$I-removal efficiency at 350–650 °C under both the KI concentrations, though the $Ag/Al_2O_3$ at $I_2$ concentrations of 166 µg/mL performed better at $< 300$ °C.

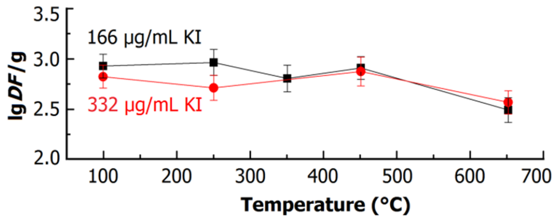

Fig. 5. (Color online) Effect of $I_2$ concentration on $^{131}$I-adsorbing performance of $Ag/Al_2O_3$ at $N_2$ flow rate of 35 mL/min.

### 3. *Effect of $N_2$ flow rate on $^{131}$I-removal efficiency*

The effect of $N_2$ flow rate on $^{131}$I-removal efficiency of adsorbents was carried out at 250 °C, with $N_2$ flow rate varying from 15 mL/min to 75 mL/min. As shown in Fig. 6, *DF* values changed little in the entire range of the $N_2$ flow rate.

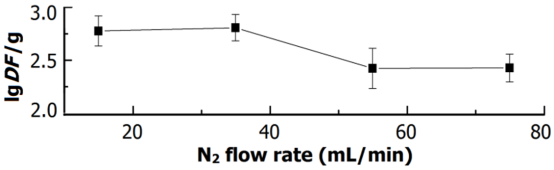

Fig. 6. Effect of $N_2$ flow rate on $^{131}$I-adsorbing performance of $Ag/Al_2O_3$ at 250 °C.

### 4. *Effect of adsorption time*

The interaction between $Ag/Al_2O_3$ and iodine was studied at 100 °C and 450 °C under $N_2$ flow rate of 35 mL/min by measuring the $^{131}$I-removal efficiency in different durations of the adsorption (Fig. 7). The *DF* value of $Ag/Al_2O_3$ increased with time till 100 min, where it reached to a plateau. Therefore, the $Ag/Al_2O_3$ can achieve desirable result of $^{131}$I-removal in adsorption time of 100 min at $N_2$ flow rate of 35 mL/min.

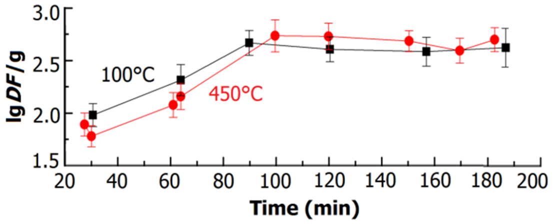

Fig. 7. (Color online) I-131 adsorption kinetics curve of $Ag/Al_2O_3$ at 100 and 450 °C under $N_2$ flow rate of 35 mL/min.

## IV. CONCLUSION

In this work, silver impregnated alumina was prepared and evaluated for its removal efficiencies of radioactive iodine at high temperatures (100, 250, 350, 450 and 650 °C). The results suggested that: alumina would perform better for adsorption radioactive iodine at high temperatures after silver loaded; the differences of removal efficiencies among different flow rates of carrier gas were small. Silver impregnated alumina would be applied as adsorbents to remove radioactive iodine at high temperatures during nuclear accident.

[1] Slovic P, Flynn J H and Layman M. Perceived risk, trust, and the politics of nuclear waste. Science, 1991, **254**: 1603–1607. DOI: 10.1126/science.254.5038.1603

[2] Bo A, Sarina S, Zheng Z F, *et al.* Removal of radioactive iodine from water using Ag2O grafted titanate nanolamina as efficient adsorbent. J Hazard Mater, 2013, **246**: 199–205. DOI: 10.1016/j.jhazmat.2012.12.008

[3] Chapin D M, Cohen K P, Davis W K, *et al.* Nuclear safety - nuclear power plants and their fuel as terrorist targets. Science, 2002, **297**: 1997–1999. DOI: 10.1126/science.1077855

[4] Burns P C, Ewing R C and Navrotsky A. Nuclear fuel in a reactor accident. Science, 2012, **335**: 1184–1188. DOI: 10.1126/science.1211285

[5] Sava D F, Rodriguez M A, Chapman K W, *et al.* Capture of volatile iodine, a gaseous fission product, by zeolitic imidazolate framework-8. J Am Chem Soc, 2011, **133**: 12398–12401. DOI: 10.1021/ja204757x

[6] Buesseler K, Aoyama M and Fukasawa M. Impacts of the Fukushima nuclear power plants on marine radioactivity. Environ Sci Technol, 2011, **45**: 9931–9935. DOI:

10.1021/es202816c

[7] Hou X L, Povinec P P, Zhang L Y, *et al.* Iodine-129 in seawater offshore Fukushima: distribution, inorganic speciation, sources, and budget. Environ Sci Technol, 2013, **47**: 3091–3098. DOI: 10.1021/es304460k

[8] Chino M, Nakayama H, Nagai H, *et al.* Preliminary estimation of release amounts of I-131 and Cs-137 accidentally discharged from the Fukushima Daiichi nuclear power plant into the atmosphere. J Nucl Sci Technol, 2011, **48**: 1129–1134. DOI: 10.1080/18811248.2011.9711799

[9] Yoshida N and Kanda J. Tracking the Fukushima radionuclides. Science, 2012, **336**: 1115–1116. DOI: 10.1126/science.1219493

[10] Kawamura H, Kobayashi T, Furuno A, *et al.* A methodology for scenario development based on understanding of long-term evolution of geological disposal systems. J Nucl Sci Technol, 2012, **48**: 1349–1356. DOI: 10.1080/00223131.2012.693884

[11] Deitz V R. Interaction of radioactive iodine gaseous species with nuclear-grade activated carbons. Carbon, 1987, **25**: 31–38. DOI: 10.1016/0008-6223(87)90037-6

[12] Chien C C, Huang Y P, Wang W C, *et al.* Efficiency of moso bamboo charcoal and activated carbon for adsorbing radioactive iodine. Clean-Soil Air Water, 2011, **39**: 103–108. DOI: 10.1002/clen.201000012

[13] Kosaka K, Asami M, Kobashigawa N, *et al.* Removal of radioactive iodine and cesium in water purification processes after an explosion at a nuclear power plant due to the Great East Japan Earthquake. Water Res, 2012, **46**: 4397-4404. DOI: 10.1016/j.watres.2012.05.055

[14] Guczi J, Angelova A, Bulman R A, *et al.* Investigation of the interactions of $^{110\mathrm{m}}\mathrm{Ag}^{+}$ and $^{125}\mathrm{I}^{-}$ with humic-acid chemically immobilized on silica-gel. Reactive Polymers, 1992, **17**: 61–68. DOI: 10.1016/0923-1137(92)90570-R

[15] Sakurai T, Takahashi A, Ye M L, *et al.* Trapping and measuring radioiodine (iodine-129) in cartridge filters. J Nucl Sci Technol, 1997, **34**: 211–216. DOI: 10.1080/18811248.1997.9733648

[16] Sarri S, Misaelides P, Noli F, *et al.* Removal of iodide from aqueous solutions by polyethylenimine-epichlorohydrin resins. J Radioanal Nucl Chem, 2013, **298**: 399–403. DOI: 10.1007/s10967-013-2662-0

[17] Usseglio S, Damin A, Scarano D, *et al.* $(I_2)(n)$ encapsulation inside $TiO_2$: A way to tune photoactivity in the visible region. J Am Chem Soc, 2007, **129**: 2822–2828. DOI: 10.1021/ja066083m

[18] Yang D J, Sarina S, Zhu H Y, *et al.* Capture of radioactive cesium and iodide ions from water by using titanate nanofibers and nanotubes. Angew Chem Int Ed, 2011, **50**: 10594–10598. DOI: 10.1002/anie.201103286

[19] Yang D J, Liu H W, Zheng Z F, *et al.* Titanate-based adsorbents for radioactive ions entrapment from water. Nanoscale, 2013, **5**: 2232–2242. DOI: 10.1039/c3nr33622k

[20] Yang D J, Liu H W, Liu L, *et al.* Silver oxide nanocrystals anchored on titanate nanotubes and nanofibers: promising candidates for entrapment of radioactive iodine anions. Nanoscale, 2013, **5**: 11011–11018. DOI: 10.1039/c3nr02412a

[21] Huang R J, Hou X L and Hoffmann T. Extensive evaluation of a diffusion denuder technique for the quantification of atmospheric stable and radioactive molecular iodine. Environ Sci Technol, 2010, **44**: 5061–5066. DOI: 10.1021/es100395p

[22] Faghihian H, Maragheh M G and Malekpour A. Adsorption of radioactive iodide by natural zeolites. J Radioanal Nucl Chem, 2002, **254**: 545–550. DOI: 10.1023/A:1021698207045

[23] Warchol J, Misaelides P, Petrus R, *et al.* Preparation and application of organo-modified zeolitic material in the removal of chromates and iodides. J Hazard Mater, 2006, **137**: 1410–1416. DOI: 10.1016/j.jhazmat.2006.04.028

[24] Watanabe Y, Ikoma T, Yamada H, *et al.* Novel long-term immobilization method for radioactive iodine-129 using a Zeolite/Apatite composite sintered body. ACS Appl Mater Interfaces, 2009, **1**: 1579–1584. DOI: 10.1021/am900251m

[25] Malik A A, Meddings P R, Patel A, *et al.* Competitive effects in the adsorption of $CH_3I$ on KI-impregnated activated carbons in the presence of $CO_2$. Carbon, 1996, **34**: 439–447. DOI: 10.1016/0008-6223(95)00165-4

[26] Kepak F. Removal of gaseous fission products by adsorption. J Radioanal Nucl Chem, 1990, **142**: 215–230. DOI: 10.1007/BF02039464

[27] Gonzalez-Garcia C M, Gonzalez J F and Roman S. Removal efficiency of radioactive methyl iodide on TEDA-impregnated activated carbons. Fuel Process Technol, 2011, **92**: 247–252. DOI: 10.1016/j.fuproc.2010.04.014

[28] Hoskins J S and Karanfil T. Removal and sequestration of iodide using silver-impregnated activated carbon. Environ Sci Technol, 2002, **36**: 784–789. DOI: 10.1021/es010972m

[29] Karanfil T, Moro E C and Serkiz S M. Development and testing of a silver chloride-impregnated activated carbon for aqueous removal and sequestration of iodide. Environ Technol, 2005, **26**: 1255–1262. DOI: 10.1080/09593332608618595

[30] Choi B S, Park G I, Lee J W, *et al.* Performance test of silver ion-exchanged zeolite for the removal of gaseous radioactive methyl iodide at high temperature condition. J Radioanal Nucl Chem, 2003, **256**: 19–26. DOI: 10.1023/A:1023383505788

[31] Garbarino G, Lagazzo A, Riani P, *et al.* Steam reforming of ethanol-phenol mixture on $Ni/Al_2O_3$: effect of Ni loading and sulphur deactivation. Appl Catal B-Environmental, 2013, **129**: 460–472. DOI: 10.1016/j.apcatb.2012.09.036

[32] Lopez-Granada G, Barceinas-Sanchez J D O, Lopez R, *et al.* High temperature stability of anatase in titania-alumina semiconductors with enhanced photodegradation of 2, 4-dichlorophenoxyacetic acid. J Hazard Mater, 2013, **263**: 84–92. DOI: 10.1016/j.jhazmat.2013.07.060

[33] Gudlur P, Muliana A and Radovic M. Effective thermo-mechanical properties of aluminum-alumina composites using numerical approach. Compos Part B-Eng, 2014, **58**: 534–543. DOI: 10.1016/j.compositesb.2013.10.052